

X-ray study of anharmonicity in AuGa₂[†]

W. C. Hollenberg* and B. W. Batterman

Department of Materials Science and Engineering, Cornell University, Ithaca, New York 14850

(Received 23 April 1974)

AuGa₂ has been studied extensively in recent years because of its rather surprising temperature-dependent Knight shift and magnetic susceptibility. To gain some information on its vibrational properties we have measured the temperature dependence of the integrated x-ray intensities of various Bragg reflections from 300 to 625 °K. We have detected the anharmonic anisotropic Ga atom vibration. The ratio of the anharmonic to harmonic potential coefficients for the Ga atom is about half that of other ionic fluorite compounds. The vibrational mean-square amplitudes of Au and Ga are found to be equal to within experimental error, while in other fluorite compounds these relative amplitudes differ by 50%. The temperature dependence of the x-ray intensities was found to be anomalously large. To fit the data a conventional quasiharmonic treatment would require a Gruneisen parameter $\gamma' = 4.6$ which is more than twice the value expected from measured expansion coefficients, specific heat, and bulk modulus. We show that this large value of γ' is most likely associated with the $C_{11} - C_{12}$ shear modulus which appears to be both volume and temperature dependent. This temperature dependence is shown to be consistent with the thermal depopulation of the high density of states just below ϵ_F and is consistent with the high-temperature Knight-shift behavior.

I. INTRODUCTION

In the past few years, much attention has been given to the isomorphous compounds AuAl₂, AuGa₂, and AuIn₂. The principal reason for this interest comes from the fact that the Ga⁷¹ Knight shift and the bulk magnetic susceptibility of AuGa₂ both display a marked temperature dependence (in fact the Knight shift changes sign at about 65 °K), whereas the corresponding quantities in AuAl₂ and AuIn₂ are almost temperature independent.¹⁻³ To further complicate matters, in contrast with these striking dissimilarities, many of the electronic properties (electronic specific heats,^{4,5} Hall coefficients,⁶ resistivities,^{6,7} magnetoresistivities,⁷ and Fermi-surface topologies⁸⁻¹¹) contain only slight differences across the series.

AuAl₂, AuGa₂, and AuIn₂ all are of the fluorite structure. In the past few years, neutron and x-ray diffraction studies of this structure have shown that certain structure factors behave in an unexpected fashion. Willis,¹² using neutron diffraction techniques to study CaF₂, first observed an unexpected temperature dependence for the integrated intensities of certain Bragg reflections. His investigations dealt with the CaF₂ [(755), (771), (933)] reflections, all of which occur at the same $(\sin\theta)/\lambda$. He showed that the Debye-Waller factors of these three reflections were different, and this result was inconsistent with thermal vibration models which assumed both the Ca and F atoms to vibrate in a centrosymmetric fashion about their equilibrium positions. Simply put, anisotropic Debye-Waller factors are inconsistent with a cubic harmonic crystal. Willis¹³ and Dawson¹⁴

were able to explain these observations quantitatively by recognizing the fact that the local site symmetry of the F atom was noncentrosymmetric, and, accordingly, by treating the problem of thermal vibrations with a phenomenological model which included anharmonic cubic and quartic terms. Since then, this approach as been used successfully to explain the results of similar investigations made with both neutrons and x-rays on different compounds with the fluorite structure. BaF₂,¹⁵ UO₂,¹⁶ and SrF₂ (Ref. 17) have been studied with neutrons, and CaF₂ (Refs. 18, 19) and Mg₂Si (Ref. 20) with x-rays.

In the present experimental study of AuGa₂, we employ Willis's model to examine quantitatively the temperature dependences of the x-ray integrated intensities for various Bragg reflections. Our goal was to see if the anharmonic anisotropic effects, which were expected to arise on account of the tetrahedral site symmetry of the Ga atom, might in some way be correlated to the unexpected behavior of the Ga⁷¹ Knight shift and bulk susceptibility of AuGa₂.

II. THEORY

AuGa₂ has the fluorite structure (see Fig. 1). The lattice is constructed from three interpenetrating face-centered-cubic sublattices; one is associated with the Au atom and two with the Ga atoms. The coordinates of the atoms are Au (*X* site): 000; Ga (*Y* site): $\frac{1}{4}\frac{1}{4}\frac{1}{4}$; and Ga (*Y'* site): $\frac{3}{4}\frac{3}{4}\frac{3}{4}$, all plus fcc translations. There are three atoms per primitive cell.

Using symmetric Bragg geometry, the total

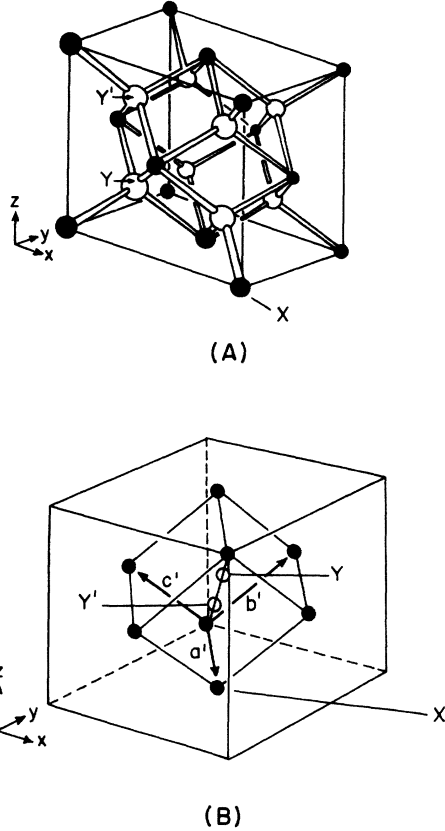


FIG. 1. Schematic representation of the fluorite structure. (a) shows all the atoms of the cubic cell. The filled circles are Au atoms and the open circles Ga in AuGa₂; (b) primitive cell, showing the environment of the two Ga-atom sites Y and Y'.

measured x-ray integrated intensity, designated as E , can be written as²¹

$$E = P_0 \frac{r_e^2 \lambda^3 \langle F \rangle \langle F^* \rangle (1 + \eta)(1 + \cos^2 2\theta)}{\omega 2\mu v_a^2 \sin 2\theta}, \quad (1)$$

where P_0 is the incident power, r_e is the classical electron radius, ω is the crystal rotation rate, λ is the x-ray wavelength (0.71 Å), μ is the linear adsorption coefficient, v_a is the volume of the unit cell, η is the thermal diffuse scattering (TDS) correction, and $\langle F \rangle$ is the structure factor. The terms μ , v_a , and $(1 + \cos^2 2\theta)/2 \sin 2\theta$ depend somewhat on temperature because of thermal expansion, and the symbol $\langle \rangle$ denotes an ensemble average.

The structure factor $\langle F \rangle$ can be written

$$\begin{aligned} \langle F \rangle = & 4(f_{\text{Au}} \langle e^{i\vec{H} \cdot \vec{u}} \rangle_X + f_{\text{Ga}} e^{i\vec{H} \cdot \vec{r}_1} \langle e^{i\vec{H} \cdot \vec{u}} \rangle_Y \\ & + f_{\text{Ga}} e^{i\vec{H} \cdot \vec{r}_2} \langle e^{i\vec{H} \cdot \vec{u}} \rangle_{Y'}) , \end{aligned} \quad (2)$$

where \vec{r}_1 , \vec{r}_2 are basis vectors $(\frac{1}{4}, \frac{1}{4}, \frac{1}{4})$ and $(\frac{3}{4}, \frac{3}{4}, \frac{3}{4})$, respectively; \vec{H} is 2π times a reciprocal lattice

vector; f_{Au} , f_{Ga} are atomic scattering factors corrected for dispersion; $\langle \rangle_i$ signifies an ensemble average evaluated at sites $i = X, Y, Y'$; \vec{u} is the time-dependent displacement of the atom from equilibrium. The problem now is to calculate the ensemble averages appearing in Eq. (1).

We adopt the formulation as developed by Willis¹³ and Dawson,¹⁴ and treat the problem classically. The motion of each atom is assumed to be determined by a local potential, and the ensemble averages are calculated using classical statistical mechanics. We deal with the Au atom first, since this case is algebraically the easiest.

The local site symmetry of the Au atom is cubic (O_h), and according to Ref. 14, we assume a local potential of the form

$$V_{\text{Au}} = V_0 + \alpha_{\text{Au}} (\frac{1}{2} r^2) - \delta_{\text{Au}} r^4, \quad (3)$$

where $r^2 = x^2 + y^2 + z^2$; x, y, z are the displacement coordinates; and V_0 , α_{Au} , and δ_{Au} are the constants of the potential. The integrals are evaluated in Ref. 13, and, neglecting high-order terms, we end up with the Debye-Waller (DW) factor

$$\begin{aligned} e^{-M_{\text{Au}}} &= \langle e^{i\vec{H} \cdot \vec{u}} \rangle_{\text{Au}} \\ &= \exp(-H^2 \frac{1}{2} kT \{ (1/\alpha_{\text{Au}} [1 + 20kT(\delta/\alpha^2)_{\text{Au}}]) \}) , \end{aligned} \quad (4)$$

where k is Boltzmann's constant.

The constants in the potential are assumed to be a function of the equilibrium volume of the crystal, and the quasiharmonic (Gruneisen) approximation¹³ is made in order to account for the fact that these constants soften as the crystal expands. We thus have, at the temperature $T = T_0 + \Delta T$, where $T_0 = 298$ °K,

$$(\Delta\alpha/\alpha)_{\text{Au}} = (\Delta\delta/\delta)_{\text{Au}} = -2\gamma\chi\Delta T, \quad (5)$$

where γ is the Gruneisen constant and χ the volume coefficient of expansion. We now let $\alpha_{0,\text{Au}}$ and $\delta_{0,\text{Au}}$ be the values of α_{Au} and δ_{Au} at temperature T_0 and substitute Eq. (5) into Eq. (4). For the temperature range in this experiment $2\gamma\chi\Delta T$ is small compared to unity and with this approximation and some algebraic manipulation we can express the bracketed $\{ \}$ term in the exponential of Eq. (4) as

$$\begin{aligned} & \frac{1}{\alpha_{\text{Au}}} \left[1 + 20kT \left(\frac{\delta}{\alpha^2} \right)_{\text{Au}} \right] \\ &= \frac{1}{\alpha_{0,\text{Au}}} \left[1 + 20kT_0 \left(\frac{\delta}{\alpha^2} \right)_{0,\text{Au}} \right] (1 + 2\gamma'\chi\Delta T), \end{aligned} \quad (6)$$

where

$$\gamma' = \gamma + 10k(\delta/\alpha^2)_{0,\text{Au}} (1 + 2\gamma\chi T_0) / \chi, \quad (7)$$

and we can write for M_{Au}

$$M_{Au} = (H^2 kT / 2\alpha_{0,Au}) \times [1 + 20kT_0(\delta/\alpha^2)_{0,Au}] (1 + 2\gamma'\chi\Delta T) . \quad (8)$$

We can put these results in a form similar to Paskin's²² reduced temperature formulation since $(1 + 2\gamma'\chi\Delta T) \approx (a/a_0)^{\delta\gamma'}$, such that now

$$M_{Au} = \frac{H^2 kT}{2\alpha_{0,Au}} [1 + 20kT_0(\delta/\alpha^2)_{0,Au}] (a/a_0)^{\delta\gamma'} , \quad (9)$$

where a and a_0 are the lattice parameters at T and T_0 , respectively. Note that in Eq. (9) the exponent contains the modified Gruneisen parameter, and if we consider the bracketed term involving δ together with $\alpha_{0,Au}$ as a modified quadratic potential coefficient, Eq. (9) is in the form of the usual reduced temperature DW factor. The modified Gruneisen parameter is defined in Eq. (7) and differs from the usual value of γ because of the expression involving the quartic term (δ) in the potential.

We can perhaps get a better insight into the significance of the quartic potential term by expressing the potential in a quasiharmonic form:

$$V_{Au} = V_0 + \frac{1}{2}\alpha'_{Au} r^2 , \quad (10)$$

where α'_{Au} is both temperature and volume dependent. The DW factor becomes from Eq. (4)

$$\exp(-M_{Au}) = \exp(-H^2 kT / 2\alpha'_{Au}) . \quad (11)$$

Assuming α'_{Au} to be weakly temperature and volume dependent we have

$$\alpha'_{Au} = \alpha'_{0,Au} + \left(\frac{\partial\alpha'_{Au}}{\partial T}\right)_0 \Delta T + \left(\frac{\partial\alpha'_{Au}}{\partial V}\right)_0 \Delta V . \quad (12)$$

If we insert Eq. (12) into Eq. (11) and treat the differential terms as small, we have for the exponent in the Debye-Waller factor

$$M_{Au} = \frac{H^2 kT}{2\alpha'_{0,Au}} \left[1 - \frac{1}{\alpha'_{0,Au}} \left(\frac{\partial\alpha'_{Au}}{\partial T}\right)_0 \Delta T - \frac{1}{\alpha'_{0,Au}} \left(\frac{\partial\alpha'_{Au}}{\partial V}\right)_0 \Delta V \right] . \quad (13)$$

If we now compare the corresponding terms in Eq. (13) with Eq. (8) we have, using Eq. (7),

$$\frac{1}{\alpha'_{0,Au}} = \frac{1}{\alpha_{0,Au}} \left[1 + 20kT_0 \left(\frac{\delta}{\alpha^2}\right)_{0,Au} \right] , \quad (14a)$$

$$\frac{1}{\alpha'_{0,Au}} \left(\frac{\partial\alpha'_{Au}}{\partial T}\right)_0 \Delta T = -20k \left(\frac{\delta}{\alpha^2}\right)_{0,Au} (1 + 2\gamma'\chi T_0) \Delta T , \quad (14b)$$

$$\frac{1}{\alpha'_{0,Au}} \left(\frac{\partial\alpha'_{Au}}{\partial V}\right)_0 \Delta T = -2\gamma'\chi \Delta T . \quad (14c)$$

Thus we see that the fourth-order term in the potential accounts for the temperature dependence of the quasiharmonic force constant α'_{Au} [Eq. (14b)], while the Gruneisen parameter γ accounts for its volume dependence. From Eq. (14a) it is clear that we can simply include the fourth-order term in the anharmonic potential in the quasiharmonic quadratic term α'_{Au} . Eqs. (14) will be important in our discussion of results.

Our model thus has Eq. (10) for the quasiharmonic local one-atom potential, along with the relationship $(\Delta\alpha'/\alpha)_{Au} = -2\gamma'\chi\Delta T$ [see Eq. (7)]. The potential parameter α' is thus considered to be both temperature and volume dependent.

Our notation can be simplified if we define some new quantities. Due to thermal expansion, $H^2 = H_0^2(a_0/a)^2$ (where the subscript zero refers to room-temperature values) and we can write

$$W_j = \frac{H_0^2 k}{2\alpha'_{0,j}} = \left(\frac{2\pi}{a_0}\right)^2 \left(\frac{k}{2\alpha'_{0,j}}\right) \sum h^2 , \quad (15)$$

$$T_2 = (a_0/a)^2 (a/a_0)^{\delta\gamma'} T , \quad (16)$$

where j refers to either Au or Ga and $\sum h^2 = h_1^2 + h_2^2 + h_3^2$. Combining Eqs. (9), (15), and (16) we have

$$M_{Au} = W_{Au} T_2 . \quad (17)$$

We next treat the Ga atom in a similar fashion. The local site symmetry of the Ga atom is tetrahedral (T_d), and we note that the local environment of one of the Ga atoms situated at the Y position is related to that of the other Ga atom situated at the Y' position by inversion. The potential associated with the two Ga atoms is

$$V_{Ga} = V_0 + \frac{1}{2}\alpha'_{Ga} r^2 \mp \beta'_{Ga}(xyz) , \quad (18)$$

with \mp for the Y and Y' sites, respectively. The ensemble averages are evaluated in Ref. 13, and the result is

$$\exp(-M_{Ga}) = \exp(-W_{Ga} T_2) \{ 1 \pm i [kT(a/a_0)^{\delta\gamma'}]^2 (2\pi/a)^3 \times (\beta'_0/\alpha'_0)^3 (h_1 h_2 h_3) \} , \quad (19)$$

where h_1, h_2, h_3 are the Miller indices, and \pm refers to Y and Y' sites, respectively. The potential parameters are assumed to be both volume and temperature dependent, and the approximation $(\Delta\alpha'/\alpha)_{Ga} = (\Delta\beta'/\beta')_{Ga} = -2\gamma'\chi\Delta T$; Eq. (7) is used here as with the Au terms.

The structure factors can now be written by substituting Eqs. (19) and (17) into Eq. (2). The structure factors for the even reflections are

$$\langle F \rangle = 4 [f_{Au} \exp(-W_{Au} T_2) \pm 2f_{Ga} \exp(-W_{Ga} T_2)] \quad (20)$$

For $\sum h = 4n$ or $4n + 2$, where $\sum h = h_1 + h_2 + h_3 = 4n$ or $4n + 2$ and require the $+$ or $-$ sign, respectively. Note that the third-order term involving β' does

not contribute to these even reflections. For odd reflections, i.e., $\sum h = 4n \pm 1$, we have

$$\begin{aligned} \langle F \rangle = & 4 \{ f_{\text{Au}} \exp(-W_{\text{Au}} T_2) \\ & \pm 2 f_{\text{Ga}} \exp(-W_{\text{Ga}} T_2) [kT(a/a_0)^{6\nu'}]^2 \\ & \times (2\pi/a)^3 (\beta'/\alpha'^3)_{0,\text{Ga}} (h_1 h_2 h_3) \} . \end{aligned} \quad (21)$$

III. EXPERIMENTAL

Symmetric Bragg geometry and ω -scan motion (moving crystal, stationary detector) were used to measure the x-ray integrated intensities. The incident zirconium-filtered Mo K_α radiation had a divergence of 0.3° , and the diffracted beam was detected with a scintillation counter coupled to a single-channel analyzer. The sample was located in a furnace which was very similar to one which has been described previously,²³ and He gas was used to ensure even heating. The sample temperature was monitored with two thermocouples, and the variation in temperature during a measurement did not exceed $\pm 0.5^\circ\text{C}$. Because of thermal expansion, the position of the Bragg reflection changed slightly with increasing temperature, and it was necessary to check to make sure that all diffracted radiation was accepted by the counter aperture as the temperature increased.

The lattice parameters from various sections of the AuGa₂ crystal were checked, and the results confirmed that the crystal was homogeneous and of a single phase. Separate sample platelets of about $10 \times 5 \times 2$ mm were prepared for each $(h_1 h_2 h_3)$ reflection measured. After each platelet was carefully oriented, it was polished so that the $(h_1 h_2 h_3)$ planes in question were parallel to the sample surface. Final polishing was done on a Syntron polishing machine, and Beuhler micro-clothes, water, and aluminum oxide powders ranging from 1 to $0.3 \mu\text{m}$ were used. The single-crystal platelet was not etched. Surface strain was partially removed by annealing the sample in a helium environment at 300°C for about three hours.

Multiple-reflection effects (Umweganregung) were checked by measuring the room-temperature integrated intensity of each sample at 90° azimuths (i.e., rotation of the crystal about a normal to the diffracting planes). The average of the 0° and 180° intensities agreed to within 2% of that corresponding to 90° – 270° azimuths. In addition, the temperature dependence of the integrated intensity was compared for a given crystal at different azimuths. These results agreed to within the statistical uncertainty. We concluded that Umweganregung effects were not present.

The linear absorption coefficient μ for AuGa₂

is about 1000 cm^{-1} . Using the atomic scattering factors and dispersion corrections given in Ref. 24 and a Debye temperature of $\Theta_x \sim 195^\circ\text{K}$,²⁵ one finds that the calculated difference between the dynamic (see Ref. 26) and kinematic integrated intensities for the AuGa₂ [975] reflection is about 5%. The polishing process left a strained surface, and since all $\sum h = 4n \pm 1$ reflections examined in the present work occurred at $(\sin\theta)/\lambda \sim 1$, these reflections were assumed to be free from extinction effects. The difference between the dynamic and kinematic integrated intensities for reflections like the (1222) was calculated to be 10% to 15%, and the crystal for each $\sum h = 4n$ reflection was purposely strained after it had been polished in order to make sure that it would behave in a kinematic fashion. Extinction errors were thus absent from all measurements.

The uncertainty due to counting statistics was less than 1.5% of the net measured integrated intensity for each data point. The incident intensity was monitored before and after each measurement, and all measurements for a given reflection were normalized to a common incident intensity. After a high-temperature run, many and sometimes all measurements were retaken; they usually agreed with the first set to within 1.5%.

The thermal expansion coefficient was needed in order to reduce the data numerically, and the Bond technique²⁷ was employed to measure the lattice constant as a function of temperature. A AuGa₂ [553] single crystal was placed inside the previously described high-temperature furnace and located at the center of a Siemens Counter Tube Goniometer. Copper K_α radiation, filtered with Ni, was used. The principal errors which occur in this experiment, as described in Ref. 27, were taken into consideration. The lattice parameter at room temperature (25°C) was $6.0757 \pm 0.002 \text{ \AA}$ and at 350°C , $6.1115 \pm 0.002 \text{ \AA}$. The average linear expansion coefficient was $(18 \pm 2) \times 10^{-6}$ over the range 25 – 350°C . The lattice parameter at 25 and 350°C agrees very well with values currently in the literature, e.g., 6.075 \AA ²⁸ and 6.078 \AA ²⁹ for 25°C and 6.117 \AA ²⁹ for 350°C .

IV. DATA ANALYSIS

Equation (20) shows that $\langle F \rangle$ for the $\sum h = 4n$ and $\sum h = 4n + 2$ reflections is a function of $\sum h^2$, whereas for the odd reflections [Eq. (21)] $\langle F \rangle$ depends on $\sum h^2$ and $(h_1 h_2 h_3)$. We consider those reflections with a common value for $\sum h^2$ but with different values of the product $(h_1 h_2 h_3)$ as belonging to a family—e.g., the reflections (971), (955), and (1131) form one family. The present model

suggests that reflections belonging to a family of odd-index reflections will have different structure factors since the product $(h_1 h_2 h_3)$ will be different for each member. All reflections belonging to an even-index family ($\sum h = 4n$), on the other hand, are expected to have the same structure factor, i.e., the even reflections will have an isotropic Debye-Waller factor.

Defining U as follows and using Eq. (1) for the experimental integrated intensity E ,

$$U = E/A(T) \approx \langle F \rangle \langle F^* \rangle, \quad (22)$$

where

$$A(T) = (1 + \eta)(1 + \cos^2 2\theta)/2 \sin(2\theta).$$

We see that a plot of U vs T should reveal whether this expected difference is there or not.

We must first calculate η , the first order TDS correction, in order to compute U . Cooper and Rouse,³⁰ assuming the first order TDS correction to be isotropic about each reciprocal lattice point, have shown how to evaluate this correction numerically. This correction depends only on $(\sin\theta)/\lambda$, the AuGa₂ elastic constants, the experimental scan range, and the temperature. The elastic constants and their temperature dependences were taken from Ref. 25, and the Cooper-Rouse FORTRAN IV program³¹ was used to perform the necessary calculation. The isotropic approximation was assumed to be sufficient (see Ref. 18, and their comments concerning the anisotropic calculation performed by Dr. C. B. Walker). For the (975) (1153) family, the scan range was 1.9°, the receiving slit range was 2.4° by 2.6°, and the correction η ranged from 15.7% at $T = 25^\circ\text{C}$ to 31.5%

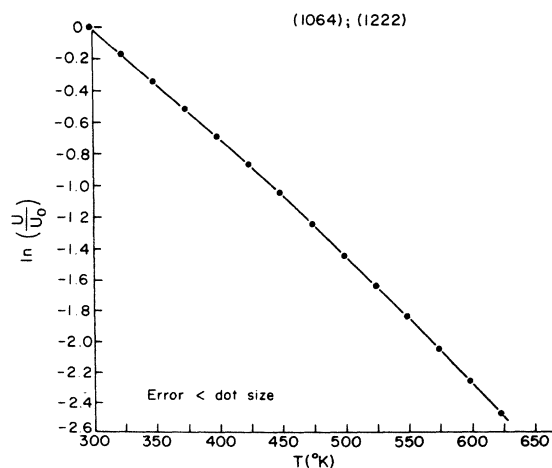


FIG. 2. Log of parameter U , proportional to integrated intensities vs absolute temperature for the (10, 6, 4) and (12, 2, 2) reflections. The points for the two separately measured intensities are coincident.

at $T = 300^\circ\text{C}$. For the (1133) (973) family and similar conditions, η was 15.9% at room temperature and 36.7% at 350°C .

Figure 2 is a plot of $\ln(U/U_0)$ vs T for the (1064) (1222) pair, and is typical of a family belonging to the $\sum h = 4n$ class. The temperature dependences of the two reflections are indistinguishable. Figure 3 shows a similar plot for two odd-reflection families, and it can be seen that members of the same family have different temperature dependences. Equation (21) predicts that $\langle F \rangle$ (and hence U) for the $\sum h = 4n + 1$ reflections should be greater than $\langle F \rangle$ for the $4n - 1$ reflections, and this is confirmed qualitatively in these graphs. The other odd-family reflections behaved similarly. The data are now interpreted in terms of Eqs. (20) and (21) in order to obtain, in a consistent fashion, the four parameters $\alpha'_{0,\text{Au}}$, $\alpha'_{0,\text{Ga}}$, $\beta'_{0,\text{Ga}}$, and γ' .

The procedure used to obtain these parameters involves successive approximations using one or more parameters to fit data sets for different classes of reflections. We outline this method in a general way.

For a first estimate of the Au DW factor

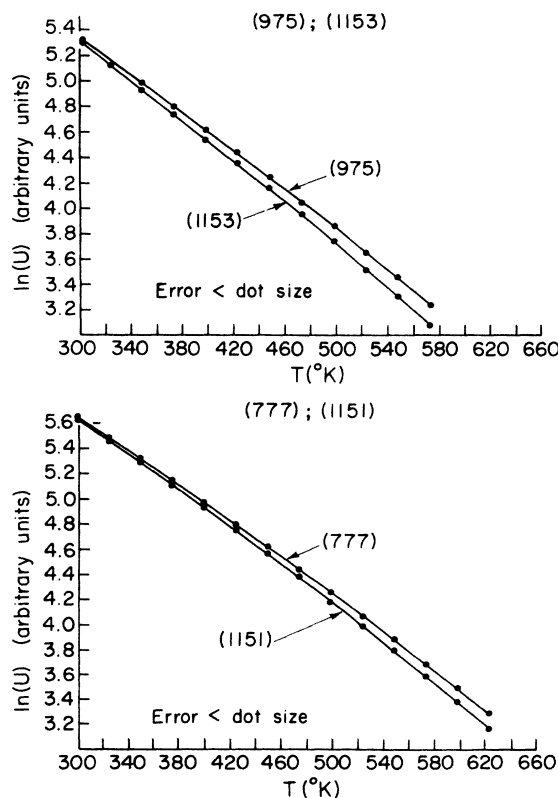


FIG. 3. Plots similar to that of Fig. 2 for two odd-reflection families. Note that the curves for each reflection within a family are different.

$\exp(-M_{Au}) = \exp(-W_{Au}T_2)$, we deal with the following odd families: (975) (1153), (777) (1151), (1133) (973), and (971) (1131) (955). From Eq. (21) one can show that the anharmonic term contributes little to the structure factor. For a first approximation we set $\beta' = 0$ and form the expression

$$P = \ln[(U_1 U_2)^{1/2} / f_{Au}^2].$$

From Eq. (21), with $\beta' = 0$, we see that $P = C_1 - 2W_{Au}T_2$; i.e., we expect P to be linear in T_2 . U_1 and U_2 are related to the two integrated intensities of two different reflections from the same family [Eq. (22)] at a given temperature, C_1 is a constant, and T_2 involves γ' [see Eqs. (7) and (8)]. Fitting P to a line linear in T_2 (using a least-squares procedure) yields W_{Au} . Consecutive values for γ' were tried until one which minimized the rms error associated with the fit was found. All odd families were analyzed in this fashion, each family producing optimum values for W_{Au} and γ' .

Now we try to improve the estimates made in the previous section. We deal directly with the two integrated intensities E_1 and E_2 , measured at temperature T (from which the numbers U_1 and U_2 were calculated in the previous section) and form

$$\ln(E_1/E_2) = \ln[(\text{const})| \langle F_1 \rangle |^2 / | \langle F_2 \rangle |^2]. \quad (23)$$

Since the two reflections belong to the same family, we see that Eq. (23) is independent of the TDS correction as well as the polarization term. Furthermore, referring to Eq. (21), we see that to a good approximation it is *proportional* to the cubic anharmonic term β' . We are dealing directly with the ratio of two experimentally measured numbers. The constant term accounts for the fact that the two data sets were taken under slightly different experimental conditions. For example, the orientation of one surface with respect to the diffracting plane was not the same as that for the other, or the surface roughness of the two specimens was not the same. The receiving slit dimensions and scan range were kept the same for both samples in order to ensure that both had identical TDS corrections. Referring to Eqs. (23) and (21) we first set $W_{Au} - W_{Ga} = 0$ (i.e., assume that the Au and Ga DW factors are the same) and do a least-squares fit on $\ln(E_1/E_2)$ for β' . Using this value of β' we recalculate P , keeping (to first-order) terms proportional to β' , and get new values for W_{Au} and γ' . All the odd-order families were investigated in this way and the values obtained lay in the ranges

$$W_{Au} / \sum h^2 = (1.98 \pm 0.04) \times 10^{-5} \text{ }^\circ\text{K}^{-1}; \quad \gamma' = 4.55 \pm 0.35. \quad (24)$$

The next step in the data refinement is to obtain an independent value for the Ga DW factor, in particular W_{Ga} . The even reflections, as can be seen from Eq. (20), depend strongly on the Ga DW factor and we consider the $\sum h = 4n$ reflections (1200) (884); (862) (1020); (1064) (1222); and (1240). With the data from a given reflection, using Eq. (20), we formed the ratio U/U_0

$$\frac{U}{U_0} = \frac{\langle F \rangle^2}{\langle F \rangle_0^2} = \left(\frac{f_{Au} e^{-W_{Au}T_2} + 2f_{Ga} e^{-W_{Ga}T_2}}{(f_{Au} e^{-W_{Au}T_2} + 2f_{Ga} e^{-W_{Ga}T_2})_0} \right)^2. \quad (25)$$

The subscript 0 refers to room temperature. Using a pair of values within the range of Eq. (24) for W_{Au} and γ' , we minimize $\{\sum_T [U/U_0 - \langle F \rangle / \langle F \rangle_0]^2\}^{1/2}$ by varying W_{Ga} . U/U_0 is calculated from the data, and $\langle F \rangle / \langle F \rangle_0$ from Eqs. (20) and (24). The resulting value for W_{Ga} together with W_{Au} and γ' was then used to calculate each data point. Experiment and calculation agreed to within 2% for all data points of a given reflection. This process was repeated for different pairs of values for W_{Au} and γ' within the range of Eq. (24). All $\sum h = 4n$ reflections were analyzed in this way, and an interpolation table was set up.

Now that we have a value for W_{Ga} , we return to the beginning, or the odd reflections. From the first part, each reflection had values for W_{Au} , γ' , and β' . We can now calculate the corresponding value for W_{Ga} from the table of the previous paragraph, and hence get $\Delta W = W_{Au} - W_{Ga}$. This final correction, which was formerly omitted, is now included in the analysis, and we arrive at improved values for W_{Au} , γ' , and β' . This process was repeated for all odd reflections. Table I shows the refined values for each odd-reflection family. With each set of the four parameters shown in the table, γ' , β' , W_{Ga} , and W_{Au} , the experimental data points were calculated using Eqs. (20) and (21). The calculated points of the reconstructed data, as a function of temperature, agreed with the experimental values to within 1%, and the resulting plots (experiment versus calculation) were indistinguishable from one another.

The success of the interactive procedure outlined above depended to some extent on the fact that large changes in β' had little effect on W_{Au} and γ' .

The temperature-dependent data from 17 reflections could be reconstructed to within 2% for all temperatures from the average parameters given below:

TABLE I. Refined values of various parameters for odd-reflection families.

Reflection	γ'	Interpolated		$\Delta W = W_{\text{Au}} - W_{\text{Ga}}$ ($^{\circ}\text{K}^{-1}$)	$10^9 \left(\frac{\beta'_0}{\alpha'_{0,3}} \right)_{\text{Ga}} k^2$ ($\text{\AA}^3 / ^{\circ}\text{K}^2$)
		$10^5 \left(\frac{W_{\text{Au}}}{\sum h^2} \right)$ ($^{\circ}\text{K}^{-1}$)	$10^5 \left(\frac{W_{\text{Ga}}}{\sum h^2} \right)$ ($^{\circ}\text{K}^{-1}$)		
(975); (1153)	$4.6 \pm 2\%$	$2.017 \pm 1.5\%$	$1.913 \pm 2\%$	$(+)0.16 \times 10^{-3}$	$0.550 \pm 3\%$
(777); (1151)	4.5	2.007	1.953	$(+)0.8 \times 10^{-4}$	0.580
(1133); (973)	4.25	2.014	2.004	$(+)0.14 \times 10^{-4}$	0.560
(971); (955)	4.85	1.946	1.967	$(-)0.26 \times 10^{-4}$	0.547
(1131); (955)	4.8	1.947	1.955	$(-)0.1 \times 10^{-4}$	0.585
Average	4.6 ± 0.4	1.986 ± 0.04	1.958 ± 0.05		0.565 ± 0.028

$$\gamma' = 4.6 \pm 0.4,$$

$$\beta'_0 = (1.58 \pm .21) \times 10^{12} \text{ erg/cm}^3,$$

$$W_{\text{Au}} / \sum h^2 = (1.99 \pm .04) \times 10^{-5} \text{ } ^{\circ}\text{K}^{-1}, \quad (26)$$

$$W_{\text{Ga}} / \sum h^2 = (1.96 \pm .05) \times 10^{-5} \text{ } ^{\circ}\text{K}^{-1},$$

$$(\beta' / \alpha')_{0,\text{Ga}} = 0.42 \pm 0.04 \text{ } \text{\AA}^{-1}.$$

In the usual notation we have

$$M_j = W_j T_2 = B_j [(\sin \theta) / \lambda]^2, \quad (27)$$

$$B_j = 8\pi^2 k / \alpha_{0,j} = 8\pi^2 \langle u_H^2 \rangle,$$

where u_H is the projection of the displacement of the j^{th} atom on the scattering vector. Thus

$$B_{\text{Au}} = 0.88 \pm 0.02 \text{ } \text{\AA}^2,$$

$$B_{\text{Ga}} = 0.867 \pm 0.02 \text{ } \text{\AA}^2.$$

An example of the reconstructed data from these parameters giving the *poorest* agreement between calculation and experiment is shown in Fig. 4. For all the other 16 reflections the agreement is even better.

For AuGa_2 , the TDS correction was quite large; for example, η [Eq. (1)] was $\sim 40\%$ at 350°C for the (777) (1151) family. If the value for η was used in the determination of any of the four parameters $\alpha'_{0,\text{Au}}$, $\alpha'_{0,\text{Ga}}$, β' , and γ' , in general it had to be known fairly accurately. This would have been especially true for the cubic anharmonic term β' , since contributions to the intensity from terms involving β' are small. However, the method employed to obtain β' involved the ratio of the integrated intensities between two members of an odd-reflection family, and hence the TDS correction was divided out. Thus, uncertainties involved in calculating β' were minimized, and we feel that the quoted accuracy of $\pm 13\%$ for β' is realistic. This method of data analysis appears to be

more accurate than that used in dealing with CaF_2 (see Ref. 18), where the quoted error in β was $\pm 33\%$.

The uncertainty in $\alpha'_{0,\text{Au}}$ and $\alpha'_{0,\text{Ga}}$, on the other hand, is determined principally by the error present in calculating the TDS correction. The numerical analysis showed that a 10% change in the value for η produced a $\sim 1\%$ change in both parameters. We estimate that the present approach used to calculate η should be accurate to $\sim 10\%$.

The x-ray Debye temperature Θ_x can be calculated from B in Eq. (27). In the Debye model⁴⁰ $B = (6h^2 T / \bar{m} k \Theta_x^2) \{F\}$. $\{F\}$ is the Debye function which is unity above 300°K , and \bar{m} is the average mass of an atom in the unit cell. Comparing B with WT_2 [Eq. (17)] we can easily show that

$$\alpha'_{0,\text{Au}} = 4\pi^2 \bar{m} k^2 \Theta_x^2 / 3h^2, \quad (28)$$

and we arrive at a Debye temperature $\Theta_x = (187 \pm 4)^{\circ}\text{K}$. This agrees well with $(192 \pm 5)^{\circ}\text{K}$ (Ref. 5) and

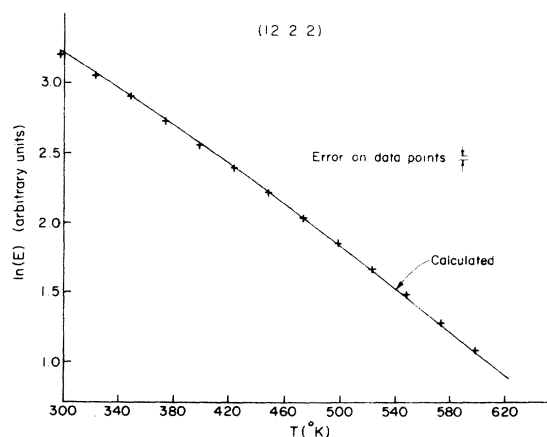


FIG. 4. Reconstruction of data for the (12, 2, 2) reflection. The solid curve is calculated using the parameters in Eq. (26) derived from the data analysis. The plus signs are the data points. This reflection is the poorest fit between calculation and experiment.

196 °K (Ref. 4) obtained from specific heat measurements and $\Theta_s = 200$ °K from Testardi's²⁵ elastic constant measurements.

Finally, using our thermal expansion coefficient, data from Ref. 25, and the usual expression for the Gruneisen parameter given in Ref. 41, we also calculate that $\gamma = 2.0$. This is less than half of what we find from our data analysis.

V. DISCUSSION OF RESULTS

From the experimental viewpoint, the temperature dependence of the integrated intensities of the Bragg reflections in AuGa₂ are quite anomalous. The most striking aspect is that the reduction in intensity with increasing temperature is much larger than one would expect using the usual quasiharmonic Gruneisen approximation. The data can be fitted with this approximation, but only if one uses an apparent Gruneisen parameter more than twice as large as one calculates from the measured expansion coefficient, specific heat, and bulk modulus.

Two other unexpected results are obtained when one compares AuGa₂ to other fluorite compounds. One is that the vibrational amplitude of Au and Ga are identical within experimental error, while for CaF₂,^{18,19} Mg₂Si,²⁰ BaF₂,¹⁵ and SrF₂,¹⁷ the mean-squared amplitudes are roughly 50% different. The other peculiarity is the fact that the third-order anharmonic potential term β' , relative to the second-order term α' , is half as large in AuGa₂ as in the other fluorite structures mentioned.

In this discussion we will attempt to relate in a semiquantitative fashion the anomalous temperature dependence to a structured electronic density of states near the Fermi energy and, further, to show that this is consistent with the observed temperature dependence of the Knight shift and elastic constants in AuGa₂.

First we discuss average sound velocities. From Testardi's²⁵ ultrasonic measurements at 400 °K, we obtain an average sound velocity \bar{v} from the bulk modulus of $\approx 2.9 \times 10^5$ cm/sec. More exactly, the sound velocities for the longitudinal modes are about 3.3×10^5 cm/sec. Those for the transverse modes are approximately 1.4×10^5 cm/sec, the $C_{11} - C_{12}$ shear mode being the softest at 1.2×10^5 cm/sec. The Debye model predicts³²

$$v = \omega_D / [6\pi^2(N_v)]^{1/3}, \quad (29)$$

where ω_D is the Debye frequency ($\hbar\omega_D = k\Theta_x$) and N_v the number of atoms per unit volume. Using $\Theta_x = 187$ °K, we get $\bar{v} \sim 1.7 \times 10^5$ cm/sec, a value quite close to that of the transverse modes.

We now calculate the long wavelength velocity v_{TF} in the Thomas-Fermi limit. Using the Thomas-Fermi approximation, it can be shown³³ that

$$v_{TF} = \omega_p \lambda_0, \quad (30)$$

where ω_p is the ionic plasma frequency and λ_0 is the Thomas-Fermi screening length. We have

$$\omega_p^2 = 4\pi(N/V)(\bar{Z}e)^2/\bar{m}, \quad (31)$$

where N/V is the number density of ions, $\bar{Z}e$ is the average valence charge, \bar{m} is the average ion mass, and

$$\frac{1}{\lambda_0^2} = 4\pi e^2 \int -\frac{\partial f}{\partial \epsilon} g(\epsilon) d\epsilon, \quad (32)$$

where $f(\epsilon)$ is the Fermi function and $g(\epsilon)$ the density of states per unit volume. Thus

$$v_{TF} = \omega_p \left(4\pi e^2 \int -\frac{\partial f}{\partial \epsilon} g(\epsilon) d\epsilon \right)^{-1/2}. \quad (33)$$

In the usual case when the density of states is slowly varying near the Fermi surface, the integral in Eq. (33) is just $g(\epsilon_F)$, the density of states at the Fermi surface. For the moment we consider this to be the case and treat the integral, and therefore $g(\epsilon_F)$, as being temperature independent. Following Rayne⁵ we use 7 electrons/molecule as the valence charge contribution (one from Au and three from each Ga). Using Rayne's low-temperature electronic specific heat⁵ we can get an approximate value for $g(\epsilon_F)$. Putting appropriate values in Eq. (33) we get $v_{TF} \approx (2-3) \times 10^5$ cm/sec, and this will depend somewhat on the strength of the electron-phonon interaction. This value is in reasonable agreement with the values obtained from the x-ray Debye temperature and the actually measured sound velocities.

Our point in these calculations is to show that an average sound velocity calculated from our experimental value of $\alpha'_{0, Au}$ is about the same as that calculated from an electron gas in the Thomas-Fermi limit. We therefore consider $\alpha'_{0, Au}$ proportional to $[\int -(\partial f/\partial \epsilon)g(\epsilon)d\epsilon]^{-1}$. In the following discussion we treat this integral as temperature dependent. From Eq. (14b) we see that the temperature dependence of this integral is related to the temperature (not volume) dependence of the quasiharmonic force constant.

Switendick and Narath³⁴ presented detailed band-structure calculations for AuAl₂, AuGa₂, and AuIn₂. In AuGa₂ the entire second band (Γ_2), lying close to but ≈ 0.012 eV below the Fermi surface, describes the s-like valence electron antibonding states between nearest-neighbor Ga atoms. It is very flat between the X and Γ points and hence represents a rather high density of states. This band is quite different in the other two iso-

structural compounds AuIn₂ and AuAl₂. Schirber,^{11,39} on the basis of experiments on the effect of pressure on the superconducting temperature and other Fermi-surface properties, concluded that these states become thermally uncovered as the temperature increases. Hence there is strong indication that the integral in Eq. (33) is temperature dependent.

We turn our attention to the anomalously large value of the Gruneisen parameter γ' . The square of the sound velocity is, in general, proportional to the corresponding elastic modulus C . From Eqs. (28) and (29) we see, then, that the quantity α' appearing in the DW exponent is proportional to the elastic moduli. It then follows that the logarithmic derivative of C and α are equal, and from the Gruneisen approximation as stated in Eq. (5)

$$(1/\alpha')(\Delta\alpha'/\Delta T) = (1/C)(\Delta C/\Delta T) = -2\gamma'\chi. \quad (34)$$

To provide a basis for comparison let us consider the logarithmic derivatives in CaF₂ and BaF₂. From the work of Wong and Schuele³⁵ we obtain the values shown in Table II. From the values of γ and χ in Table II we see that $-2\gamma\chi$ is of the order of $-2.1 \times 10^{-4} \text{ }^\circ\text{K}^{-1}$ and $-(1.8-2.3) \times 10^{-4} \text{ }^\circ\text{K}^{-1}$ for CaF₂ and BaF₂, respectively. We note there is reasonably good agreement between the logarithmic temperature derivative of the elastic moduli and the value for $-2\gamma\chi$. The situation is

TABLE II. Logarithmic derivatives of the elastic constant for CaF₂, BaF₂, and AuGa₂ from Refs. (35) and (25), together with corresponding values of the Gruneisen parameter γ and the thermal expansion coefficient χ .

	CaF ₂	BaF ₂	AuGa ₂
$-\frac{1}{C_{11}} \frac{dC_{11}}{dT}$	2	2.2	2
$-\frac{1}{C_{12}} \frac{dC_{12}}{dT}$	2.6	3.2	1
$-\frac{1}{C_{11}-C_{12}} \frac{d(C_{11}-C_{12})}{dT}$	1.8	1.5	4.4
$-\frac{1}{C_{44}} \frac{dC_{44}}{dT}$	3.5	2.9	2
$-\frac{1}{C_{11}+2C_{12}}$	2.1	2.7	1.4
γ	1.9	1.6-2.1 ^a	4.6 ^b 2.0 ^c
$\chi(10^{-6} \text{ }^\circ\text{K}^{-1})$	56.4	54.9	54.0
$2\gamma\chi(10^{-4} \text{ }^\circ\text{K}^{-1})$	2.1	1.8-2.3	5.0 ^b 2.2 ^c

^aSee Ref. 13.

^cCalculated.

^bFrom data analysis.

different for AuGa₂, as can be seen in column 3 of the table. The logarithmic derivative for $C_{11} - C_{12}$ ranges from two to four times the values for the other AuGa₂ moduli. We have shown earlier [Eq. (14)] that the total derivative of α' with temperature can be separated into explicit volume- and temperature-dependent terms:

$$\frac{1}{\alpha'_0} \frac{\Delta\alpha'}{\Delta T} = \frac{1}{\alpha'_0} \left(\frac{\partial\alpha'}{\partial V} \right)_0 \frac{\partial V}{\partial T} + \frac{1}{\alpha'_0} \left(\frac{\partial\alpha'}{\partial T} \right)_0 = -2\gamma'\chi. \quad (35)$$

Numerically this is $\approx -(5.0 \pm 0.4) \times 10^{-4} \text{ }^\circ\text{K}^{-1}$ and is close to the value for the logarithmic derivative of $C_{11} - C_{12}$. The first term in Eq. (35) is the explicit volume dependence of the quasi-harmonic force constant, and this is $-2\gamma\chi = -2.2 \times 10^{-4} \text{ }^\circ\text{K}^{-1}$ (note that γ , not γ' , is involved). This compares favorably to the values for the other moduli shown in Table II. The difference between 5.0×10^{-4} and 2.2×10^{-4} , i.e., 2.8×10^{-4} , is the contribution from the *explicit* temperature dependence of the elastic modulus in question. Also remember that the sound velocity calculated with the Debye model (recall that ω_D^2 is proportional to α') was shown to be quite close to that of the $C_{11} - C_{12}$ shear mode, and that this is the softest mode. We would thus like to associate the unexpectedly high value for the apparent Gruneisen parameter with the temperature dependence of the $C_{11} - C_{12}$ shear modulus. We also note recent work (see, for example, Sham³⁶ or Rehwald *et al.*³⁷) dealing with compounds which have a sharp peak in the electronic density of states just below the Fermi energy. Sham has shown that this peculiarity produces a situation in which some of the elastic moduli are both volume and temperature dependent (the moduli are usually only volume dependent). In the present case, since we have attributed the large value of γ' to the $C_{11} - C_{12}$ elastic modulus, and since γ' contains a term which describes the temperature dependence of this modulus, it appears as if $C_{11} - C_{12}$ is both volume and temperature dependent, and hence probably most sensitive to the thermal depopulation of the high density of states region just beneath ϵ_F . The numerical work of the last paragraph suggests that the remaining moduli, on the other hand, are principally volume dependent and relatively insensitive to this thermal effect. We now speculate on the relationship between the foregoing arguments and the Ga⁷¹ Knight shift in the 300-600 °K range. From the Jaccarino *et al.*¹ and Warren *et al.*²⁹ measurements, the Knight shift is positive in this range. From Fig. 1 of Ref. 1, we find that the logarithmic derivative $K_n^{-1}(\Delta K_n/\Delta T) \approx (2.4 \pm 0.5) \times 10^{-4} \text{ }^\circ\text{K}^{-1}$ and from Table I of Ref. 26, the same

derivative is $\sim (1.7 \pm 0.5) \times 10^{-4} \text{ }^\circ\text{K}^{-1}$. The Knight shift behavior in this range is *s* contact in nature, and is thus proportional to³⁸ $\int -(\partial f / \partial \epsilon) g(\epsilon) d\epsilon$. We have suggested that the temperature dependence of the quasiharmonic force constant is proportional to the inverse of this integral. [From Eqs. (28) and (29), v^2 is proportional to α' , which is inversely proportional to the integral.] It follows readily that

$$\frac{1}{\alpha'_0} \frac{\partial \alpha'_0}{\partial T} \approx \frac{1}{K_n} \frac{\Delta K_n}{\Delta T},$$

where the logarithmic derivative of α'_0 refers to the explicit temperature dependence, which, from Eq. (35), is

$$-2(\gamma' - \gamma)\chi \approx - (2.8 \pm 0.5) \times 10^{-4} \text{ }^\circ\text{K}^{-1}.$$

This is in surprisingly good agreement with the measured Knight shift value of $\sim (2.0 \pm 0.5) \times 10^{-4} \text{ }^\circ\text{K}^{-1}$. Admittedly the argument is *not* very rigorous, but it does support the contention that the large value of γ' needed to explain the strong temperature dependence of the x-ray integrated intensities in AuGa₂ is due to the thermal uncovering of the density of states just below the Fermi energy.

The explicit anharmonic parameter β'_{Ga} , the third-order term in the one-atom potential, is not as easily discussed in a semiquantitative fashion. The ratio $\beta'_{\text{Ga}}/\alpha'_{\text{Ga}}$ is a measure of the degree of anisotropic motion relative to the quasiharmonic vibration. For the XY_2 ionic fluorite compounds such as CaF₂, Mg₂Si, BaF₂, SrF₂, $(\beta/\alpha)_y \approx 1 \text{ } \text{Å}^{-1}$ while for $(\beta'/\alpha')_{\text{Ga}}$ we have $\approx 0.4 \text{ } \text{Å}^{-1}$. On the other hand the relative mean-square amplitude of the X to Y atoms in the ionic compounds is ≈ 1.5 , while the Au and Ga amplitudes are the same in AuGa₂. Thus, in AuGa₂, there seems to be a greater tendency for the Au and Ga vibrations to be coupled. It appears that the noncentrosymmetric nature of the Ga atomic motion is much weaker in AuGa₂ than in the other compounds mentioned above. The rather weak noncentrosymmetric Ga motion also suggests that the optic modes contribute very little to the DW factor.

VI. SUMMARY AND CONCLUSIONS

The present experimental study of AuGa₂ has dealt with the temperature dependence, in the range 300–625 °K, of the x-ray integrated intensities for various Bragg reflections. This compound has the fluorite (XY_2) structure, and the local environment of the Ga atom is tetrahedral in nature. If one treats the problem of thermal vibrations with an Einstein single-atom potential model which includes this tetrahedral symmetry,

one expects the odd-index reflections (i.e., those for which $h+k+l=4n+1$) to have structure factors which are not isotropic. Willis,¹² while studying CaF₂, was the first to notice this anisotropy, and Dawson¹⁴ and Willis¹³ developed a local potential model to quantitatively explain these observations. This approach has since been used successfully to explain similar effects in other ionic fluorite crystals.^{15–20} In the present study, the odd-index reflections were observed to behave in the expected anisotropic fashion, and the temperature dependence of all integrated intensities was successfully accounted for with the Dawson-Willis model.

Using this approach, one finds that the atomic mean-square vibrational amplitude is inversely proportional to the quasiharmonic (quadratic) force constant α' . The anisotropic nature of the odd-index reflections is expressible in terms of a parameter $(\beta'_0/\alpha'_0)_{\text{Ga}}$, where β' is the coefficient of the third-order term in the Ga local potential. We considered the potential parameters to be both volume and temperature dependent, since this allows one to neglect possible fourth-order terms.

The experimental results turned out to be quite anomalous, particularly when compared with those of other fluorite structures. The mean-square vibrational amplitudes for Au and Ga were found to be equal to within experimental error. In the other fluorite compounds studied, these amplitudes differed by about 50%. In addition, the anisotropic parameter $(\beta'/\alpha')_{\text{Ga}}$ was one-half as large in AuGa₂ as in the other compounds mentioned above. We interpret this to indicate that the motion of the Ga atom is coupled to that of the Au atom to a much greater extent than is the motion of the Y atom to that of the X atom in the other examples. The noncentrosymmetric nature of the Ga atomic motion is much weaker here.

In addition, the rate at which all integrated intensities decreased with increasing temperature was much greater than expected. An apparent Gruneisen parameter γ' of 4.6 was needed in order to fit the data, using the conventional quasiharmonic treatment. This is more than twice the value one calculates from the measured expansion coefficient, specific heat, and bulk modulus. To attempt to explain this we first noted that recent work (see Refs. 34–36) has shown that one can expect compounds which have a sharp peak in the electronic density of states just below the Fermi energy (AuGa₂ is such a compound) to have some elastic moduli which are both volume and temperature dependent. Within the present model, γ' was used to describe the explicit volume and temperature dependence of α' . We also showed that the logarithmic derivative of α' , $(1/\alpha')(\Delta\alpha'/\Delta T)$, was approximately that of the $C_{11} - C_{12}$ shear mod-

ulus. The high value for γ' was associated with the temperature dependence of this modulus, and we conclude that it appears likely that this modulus is both volume and temperature dependent. It

is probably most sensitive to the thermal depopulation of the high density of states region just beneath ϵ_F . The remaining moduli seem to be insensitive to this thermal effect.

†Work supported by the Advance Research Projects Agency through the Materials Science Center of Cornell University.

*Paper based on research performed by W. C. Hollenberg for the Ph.D. degree, 1974. Present address: Universität Dortmund, Institut für Physik, 46 Dortmund-Hombruch, Postfach 500, West Germany.

¹V. Jaccarino *et al.*, Phys. Rev. Lett. 21, 1811 (1968).

²A. C. Switendick and A. Narath, Phys. Rev. Lett. 22, 1423 (1969).

³G. C. Carter, I. D. Weisman, L. H. Bennett, and R. E. Watson, Phys. Rev. B 5, 3621 (1972).

⁴J. H. Wernick, A. Meth. T. H. Geballe, G. Hull, and J. P. Maita, Phys. Chem. Solids 30, 1949 (1969).

⁵J. A. Rayne, Phys. Lett. 7, 114 (1963).

⁶J. P. Jan and W. B. Pearson, Philos. Mag. 8, 279 (1963).

⁷J. T. Longo, P. A. Schroeder, and D. J. Sellmyer, Phys. Rev. 182, 658 (1969).

⁸J. P. Jan, W. B. Pearson, Y. Saito, M. Springford, and I. M. Templeton, Philos. Mag. 12, 1271 (1965).

⁹J. T. Longo *et al.*, Phys. Rev. 187, 1185 (1969).

¹⁰J. E. Schirber and A. C. Switendick, Solid State Commun. 8, 1383 (1970).

¹¹J. E. Schirber, Phys. Rev. B 6, 333 (1972); Phys. Rev. Lett. 28, 1127 (1972).

¹²B. T. M. Willis, Acta Crystallogr. 18, 75 (1965).

¹³B. T. M. Willis, Acta Crystallogr. A 25, 277 (1969).

¹⁴B. Dawson, Proc. R. Soc. Lond. A 298, 255 (1967).

¹⁵M. J. Cooper, K. D. Rouse, and B. T. M. Willis, Acta Crystallogr. A 24, 484 (1968).

¹⁶K. D. Rouse, B. T. M. Willis, and A. W. Pryor, Acta Crystallogr. B 24, 117 (1968).

¹⁷M. J. Cooper and K. D. Rouse, Acta Crystallogr. A 27, 622 (1971).

¹⁸H. Strock and B. Batterman, Phys. Rev. B 5, 2337 (1972).

¹⁹M. J. Cooper, Acta Crystallogr. A 26, 208 (1970).

²⁰M. J. Cooper and D. Panke, Acta Crystallogr. A 26, 292 (1970).

²¹B. E. Warren, *X-Ray Diffraction* (Addison-Wesley, Reading, Mass., 1969), p. 46.

²²A. Paskin, Acta Crystallogr. 10, 667 (1957).

²³B. W. Batterman, Phys. Rev. 126, 1461 (1962).

²⁴*International Tables for X-Ray Crystallography* (Kynoch, Birmingham, England, 1962), Vol. 3.

²⁵L. R. Testardi, Phys. Rev. B 1, 4851 (1970).

²⁶J. J. DeMarco and R. J. Weiss, Acta Crystallogr. 19, 68 (1965).

²⁷W. L. Bond, Acta Crystallogr. 13, 814 (1960).

²⁸W. B. Pearson, *Handbook of Lattice Spacings and Structures of Metals* (Pergamon, New York, 1967), Vol. 2.

²⁹W. W. Warren, Jr., R. W. Shaw, Jr., A. Meth, F. J. DiSalvo, A. R. Storm, and J. H. Wernick, Phys. Rev. B 7, 1247 (1973).

³⁰M. J. Cooper and K. D. Rouse, Acta Crystallogr. A 24, 405 (1968); 25, 615 (1969).

³¹K. D. Rouse and M. J. Cooper, Harwell Research Group Report No. AERE-R5725, 1968 (unpublished).

³²F. Reif, *Fundamentals of Statistical and Thermal Physics* (McGraw-Hill, New York, 1965), p. 415.

³³J. M. Ziman, *Principles of the Theory of Solids* (Cambridge U.P., Cambridge, England, 1964), Chap. 6.

³⁴A. C. Switendick and A. Narath, Phys. Rev. Lett. 22, 1423 (1969).

³⁵C. Worz and D. E. Schuele, J. Phys. Chem. Solids 29, 1309 (1968).

³⁶L. J. Sham, Phys. Rev. B 6, 3581 (1972); 6, 3584 (1972); Phys. Rev. Lett. 27, 1725 (1971).

³⁷W. Rehwald, M. Rayl, R. W. Cohen and G. D. Cody, Phys. Rev. B 6, 363 (1972).

³⁸C. P. Slichter, *Principles of Magnetic Resonance* (Harper and Row, New York, 1963), p. 97.

³⁹T. F. Smith, R. N. Shelton, and J. E. Schirber, Phys. Rev. B 8, 3479 (1973).

⁴⁰R. W. James, *Optical Principles of the Diffraction of X-Rays* (Bell, London, 1950), p. 219.

⁴¹C. Kittel, *Introduction to Solid State Physics* (Wiley, New York, 1966), p. 183.